

See discussions, stats, and author profiles for this publication at: <https://www.researchgate.net/publication/8977433>

# Epitaxial Electrodeposition of Prussian Blue Thin Films on Single-Crystal Au(110)

ARTICLE *in* JOURNAL OF THE AMERICAN CHEMICAL SOCIETY · JANUARY 2004

Impact Factor: 12.11 · DOI: 10.1021/ja0381151 · Source: PubMed

CITATIONS

25

READS

54

5 AUTHORS, INCLUDING:



**Shuji Nakanishi**

Osaka University

84 PUBLICATIONS 1,039 CITATIONS

SEE PROFILE



**Guotao Lu**

8 PUBLICATIONS 85 CITATIONS

SEE PROFILE



**Jay A. Switzer**

Missouri University of Science and Technology

123 PUBLICATIONS 3,341 CITATIONS

SEE PROFILE

## Epitaxial Electrodeposition of Prussian Blue Thin Films on Single-Crystal Au(110)

Shuji Nakanishi, Guotao Lu, Hiten M. Kothari, Eric W. Bohannon, and Jay A. Switzer\*

Department of Chemistry and Graduate Center for Materials Research, University Missouri-Rolla, Rolla, Missouri 65409-1170

Received August 25, 2003; E-mail: jswitzer@umr.edu

Thin films of Prussian blue (PB),  $\text{Fe}^{\text{III}}_4[\text{Fe}^{\text{II}}(\text{CN})_6]_3$ , and its analogues have received a lot of attention as molecular magnetic materials in recent years. Various novel magnetic properties have been found in these materials as summarized in recent reviews.<sup>1</sup> For example,  $\text{V}[\text{Cr}(\text{CN})_6]_{0.86}2.8\text{H}_2\text{O}$  exhibits a greater than room-temperature  $T_c$  value (315 K)<sup>2</sup> and  $\text{K}_{0.2}\text{Co}_{1.4}[\text{Fe}(\text{CN})_6]_6\text{H}_2\text{O}$  shows photoinduced reversible magnetization.<sup>3</sup> By preparing epitaxial films of these molecular magnetic materials, it will be possible to determine orientation-dependent properties of the materials. This is presently not possible with polycrystalline or amorphous films. It will also open the door to the development of novel molecular spintronic devices, such as those which exhibit spin-dependent electron transfer.

Epitaxial electrodeposition has been demonstrated for a number of metal oxides on single-crystal metal<sup>4–7</sup> and semiconductor<sup>8–10</sup> substrates. A common feature in our earlier work is that the systems typically had large lattice mismatch, which was reduced by the formation of coincidence lattices. Here we show that it is possible to electrodeposit epitaxial PB films on a single-crystal Au(110) substrate, in which there is also a very large lattice mismatch of 148%.

The crystal structure of PB was originally proposed by Keggin and Miles<sup>11</sup> and has been modified by Herren et al. by a neutron-diffraction study.<sup>12</sup> PB has a cubic face-centered structure with a lattice parameter of 10.13 Å, consisting of alternating Fe(II) and Fe(III) located on a face-centered cubic lattice, in which Fe(II) atoms are linked to the carbon of the cyanide ions and Fe(III) atoms are linked to the nitrogen atoms. PB thin films can be prepared chemically or electrochemically from aqueous solutions containing ferric and ferricyanide ions. The preparation of thin PB film on conducting substrates was first reported by Neff.<sup>13</sup> The PB films were deposited by simply inserting clean electrodes, such as Pt, Au, and Ag, in the ferric–ferricyanide solution. Electrochemical preparation of PB was introduced by Itaya et al., which enabled the deposition of thicker films on various kinds of substrates.<sup>14</sup>

PB thin films were deposited using the method developed by Itaya et al.<sup>14</sup> The deposition bath consisted of 0.5 mM  $\text{K}_3\text{Fe}(\text{CN})_6$  and 0.5 mM  $\text{Fe}(\text{NO}_3)_3$  in 0.25 M KCl as supporting electrolyte prepared with HPLC-grade water (Aldrich). All the other chemicals were reagent-grade. The solution was maintained at room temperature. Prior to electrodeposition, the Au substrate was electrochemically polished at a constant anodic current density of  $1.6 \text{ Acm}^{-2}$  in a solution containing 25 vol % ethylene glycol, 25 vol % HCl, and 50 vol % ethanol with a graphite counter electrode. The electrode surface was annealed in a  $\text{H}_2$  flame just before the PB electrodeposition. The epitaxial PB film was grown by applying a constant potential (+0.3 V vs SCE). The working electrode consisted of a 1-cm diameter Au(110) single crystal, which was purchased from Monocrystals Company. An SCE and a platinum wire were used as reference and counter electrodes, respectively. X-ray pole figures

were run on a Philips X'pert Materials Research Diffractometer system. The surface morphology of the films was observed with a Hitachi S4700 cold field emission scanning electron microscope (SEM).

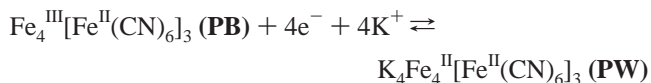
Figure 1A is the pole figure for the PB film, which shows both the out-of-plane and in-plane orientations of the film. The pole figure was acquired by setting  $2\theta$  for a plane that is not parallel with the surface. The  $2\theta$  angle was set at  $17.510^\circ$  for Figure 1A, which is the angle for (200) diffraction of PB. The tilt angle,  $\chi$ , was varied from  $0$  to  $90^\circ$  while azimuthally rotating the sample from  $\phi = 0$ – $360^\circ$ . The (200) pole figure has six peaks at the tilt angle,  $\chi$ , of  $54.7^\circ$  (the angle between (111) and (200) for a cubic structure), which means the PB film has a [111] out-of-plane orientation. The [111]-oriented film has a different out-of-plane orientation than the Au(110) substrate. Each [111] epitaxial domain of PB should give three peaks at  $\chi = 54.7^\circ$  on the (200) pole figure because of its three-fold symmetry. Therefore, the six peaks indicate that there are two epitaxial domains of PB. This result clearly shows that the PB film has both out-of-plane and in-plane orientations.

The in-plane orientation of the film relative to the Au substrate is determined by comparing the pole figures for the PB film and the Au substrate. Figure 1B shows the (200) pole figure for the Au(110) substrate, on which two peaks appear at  $\chi = 45.0^\circ$  (the angle between (110) and (200)). From the comparison between Figure 1, A and B, it is seen that the angles between the  $[\bar{1}2\bar{1}]$  axis of the PB and the  $[\bar{1}10]$  axis of the Au(110) are  $\pm 30^\circ$ .

Figure 2 shows an SEM image of the PB film. It can be seen that there are aligned pyramidal structures on the surface. As expected from the XRD experiment shown in Figure 1, two kinds of pyramidal structures with a  $60^\circ$  rotation ( $\pm 30^\circ$  rotation relative to the substrate) are observed.

There are two kinds of epitaxial domains that are rotated  $60^\circ$  relative to each other. The epitaxial relationships can be expressed as  $(1 \times 2)\text{PB}(111)[\bar{1}10]/(6 \times 5)\text{Au}(110)[\bar{1}10]$  and  $(1 \times 2)\text{PB}(111)[01\bar{1}]/(6 \times 5)\text{Au}(110)[\bar{1}10]$ . An interface model for one of the epitaxial relationships is shown in Figure 3. The lattice mismatches along the  $[\bar{1}12]$  and  $[\bar{1}10]$  directions of PB are 1.4 and  $-0.7\%$ , respectively.

It is well-known that PB films on conducting materials show electrochemical redox peaks originating from the PB and Prussian white (PW) reversible transformation in aqueous solution with particular cations, such as potassium ions. The reaction can be expressed as below.



The redox reactions require the migration of potassium ions inside the film to compensate charge. The solid curve in Figure 4 shows a cyclic voltammogram (CV) in 0.1 M  $\text{K}_2\text{SO}_4$  solution

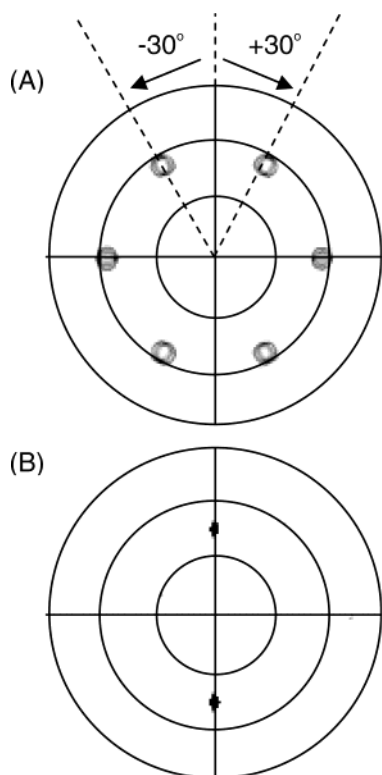


**Figure 1.** (200) pole figures for (A) PB film and (B) Au(110). The radial grid lines on the pole figure correspond to 30° increments of the tilt angle. The six spots at  $\chi = 55^\circ$  in (A) and two spots in (B) at  $\chi = 45^\circ$  correspond to the angles between the (200) and (111), and the (200) and (110) planes, respectively.

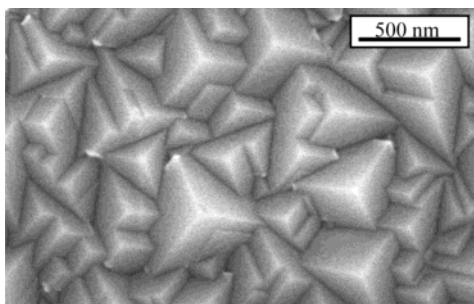


**Figure 2.** SEM image of the epitaxial PB film. Two domains of pyramidal structures with a 60° rotation relative to each other are clearly seen.

obtained for the epitaxial PB film grown on the Au(110) substrate with a deposition time of 60 min at +0.3 V. It can be seen that there are redox peaks at about +0.2 V due to the PB–PW transformation. The dashed curve shows the CV for the polycrystalline PB film grown on the polycrystalline Au substrate. The CV for the epitaxial PB film shows sharper peaks than those for the polycrystalline film. We attribute the increased sharpness for the epitaxial film to higher order in the film and to the existence of a single out-of-plane orientation. The highly ordered structure may lead to less dispersion among the possible transport paths for  $K^+$ .

In summary, we have shown that it is possible to electrodeposit an epitaxial PB film onto a single-crystal Au(110) substrate. Because of the large lattice mismatch of the PB/Au system, the PB film had a different out-of-plane orientation ([111] out-of-plane orienta-

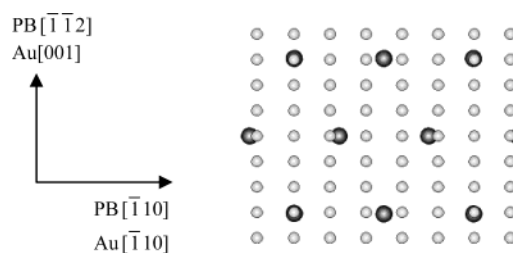


**Figure 3.** Schematic illustration of the epitaxial relationship. The values of the lattice mismatches are 1.4 and –0.7% in the  $[1\bar{1}2]$  and  $[110]$  directions of PB, respectively. Au atoms are light, Fe(III) atoms in the PB structure are dark. The other elements in PB, Fe(II), N, and C, are not shown for clarity.

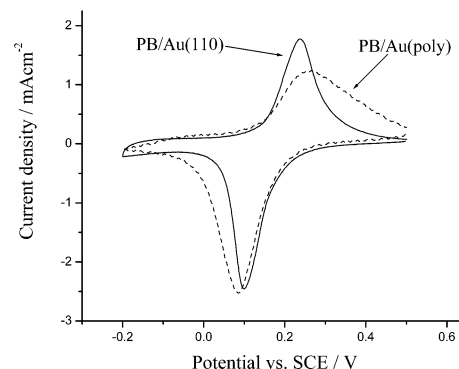


**Figure 4.** Cyclic voltammograms of the epitaxial PB film on Au(110) substrate (solid line) and the polycrystalline PB film deposited on polycrystalline Au substrate (dashed line) in 0.1 M  $K_2SO_4$  solution at 20 mV/s. Both of the PB films were deposited at +0.3 V vs. SCE for 60 min.

tion) than the Au(110) substrate. We expect that epitaxial electrodeposition will be applicable to the other PB analogues on various kinds of substrates, such as half-metallic materials such as  $Fe_3O_4$ ,<sup>5</sup> which may work as novel devices with spin-dependent electron transfer.

**Acknowledgment.** This work was supported by NSF Grants CHE-0243424, DMR-0071365, and DMR-0076338, the University of Missouri Research Board, and the Department of Energy.

## References

- (1) (a) Miller, J. S. *Electrochem. Soc. Interface* **2002**, *11*, 22–27. (b) Verdager, M.; Galvez, N.; Garde, R.; Desplanches, C. *Electrochem. Soc. Interface* **2002**, *11*, 28–32. (c) Ohkoshi, S.; Hashimoto, K. *Electrochem. Soc. Interface* **2002**, *11*, 34–38.
- (2) Ferlay, S.; Mallah, T.; Ouahes, R.; Veillet, P.; Verdager, M. *Nature* **1995**, *378*, 701.
- (3) Sato, O.; Iyoda, T.; Fujishima, A.; Hashimoto, K. *Science* **1996**, *272*, 704.
- (4) Switzer, J. A.; Shumsky, M. G.; Bohannon, E. W. *Science* **1999**, *284*, 293.
- (5) Sorenson, T. A.; Morton, S. A.; Waddill, G. D.; Switzer, J. A. *J. Am. Chem. Soc.* **2002**, *124*, 7604.
- (6) Bohannon, E. W.; Shumsky, M. G.; Switzer, J. A. *Chem. Mater.* **1999**, *11*, 2289.
- (7) Switzer, J. A.; Kothari, H. M.; Poizot, P.; Nakanishi, S.; Bohannon, E. W. *Nature* **2003**, *425*, 490.
- (8) Switzer, J. A.; Liu, R.; Bohannon, E. W.; Ernst, F. J. *Phys. Chem. B* **2002**, *106*, 12369.
- (9) Pauporte, Th.; Lincot, D. *Appl. Phys. Lett.* **1999**, *75*, 3817.
- (10) Pauporte, Th.; Cortes, R.; Froment, M.; Beaumont, B.; Lincot, D. *Chem. Mater.* **2002**, *14*, 4702.
- (11) Keggin, J. F.; Miles, F. D. *Nature* **1936**, *137*, 577.
- (12) Herren, F.; Fischer, P.; Ludi, A.; Hälg, W. *Inorg. Chem.* **1980**, *19*, 956.
- (13) Neff, V. D. *J. Electrochem. Soc.* **1978**, *125*, 886.
- (14) Itaya, K.; Uchida, I.; Neff, V. D. *Acc. Chem. Res.* **1986**, *19*, 162.

JA0381151